

# Observing Lockdown from the Outer Space

Jin Niu\*

Advisor: Prof. Florian Gunsilius

April 8, 2023

## Abstract

I examine how nighttime lights captured by satellites respond to the government-enforced lockdown policies during the COVID-19 pandemic in 2020. Milan, Italy is chosen as the treatment unit, and distributional synthetic control is used with nine control units to construct counterfactual Milan supposing it had not gone through any lockdown in 2020. I find there is a difference in night light luminosity between treated Milan and counterfactual Milan, but this difference is not significant from a placebo permutation test. After conducting similar analysis on GDP per capita for Italy with three control countries, I find no evidence suggesting the lockdown policy had a significant effect on GDP per capita. The findings reveal that during the global pandemic, the government-enforced lockdown policy in Italy did not have a considerable impact on the night light luminosity, which aligns with the economic outcome when compared to regions without such enforced policies.

---

\*Department of Economics, University of Michigan, Ann Arbor (email: [jinniu@umich.edu](mailto:jinniu@umich.edu))

# 1 Introduction

Economists have been exploring alternative indicators for gauging economic activity beyond the commonly used GDP. One such alternative is the luminosity of night lights in urban areas. Intuitively, a more developed region has higher energy consumption, denser buildings, more transportation networks and more economic activities, resulting in a more illuminated area as observed from the outer space. This paper is concerned with examining how night lights, as an indicator of economic performance, respond to lockdown policies that are enforced by the government in cities during the global pandemic in 2020. The findings indicate that the luminosity of night lights in the treatment unit did not undergo significant changes due to the implementation of lockdown policies, which is in line with the outcome of quarterly GDP.

The motivation of using night lights over other measures to study the impact of the lockdown policy is that other measures are often not consistently available, not available at a subnational level, or not updated timely. The satellite image of night lights is generated on a monthly basis and readily available where natural weather allows. The luminosity is quantified in digital numbers assigned to each pixel in the image, whose measure remains consistent over time. Another advantage of using night lights is the ability to analyze economic activity at a more localized level that is not constrained by data reporting agents, whereas GDP is usually reported on country levels. [Henderson et al. \(2012\)](#) investigated the relationship between changes in night lights intensity and real income growth. Specifically, they show that as income levels increase, there is a corresponding increase in per capita light usage, resulting in an increase in the brightness of night lights. Using night lights as an additional measure of income growth, they obtained a best-fit elasticity model of measured GDP growth ( $\Delta \ln(\text{GDP})$ ) with respect to lights growth ( $\Delta \ln(\text{lights/area})$ ), and find that the estimated elasticity is roughly 0.3 and significant at the 1% level. Moreover, night lights respond to economic downturns as well as growth. They found that the digital number representing light luminosity in Indonesia declined by 6 percent during the Asian financial crisis when GDP decreased by 13 percent. Also, Kigali, the capital of Rwanda, underwent a sharp temporary dimming from 1993 to 1994 during the Rwandan Genocide. The primary idea of this paper when using night light luminosity as an indicator of economic fluctuations is based on the positive correlation between GDP growth and change in brightness of night lights established by [Henderson et al. \(2012\)](#).

The COVID-19 global pandemic emerged in the light of 2020, and the government-issued lockdown policies to curb the spread of COVID-19 incurred some degree of hiatus on industries of all levels from manufacturing, transportation to sales and services, which led to decrease in countries' GDP and increase in unemployment rates. A study by [Chetty et al. \(2020\)](#) investigated the pandemic's impact on people's spending behaviors and the labor market in different wage levels using public database from private companies that track consumer spending, business revenues, et cetera. They observed that high-income groups reduced spending significantly, which led to substantial decrease in revenue for small businesses in affluent, dense areas that rely on in-person

interactions. As a result, those businesses laid off employees, leading to widespread and persistent low employment rates in the affected areas, particularly for low-wage workers. [Dingel and Neiman \(2020\)](#) evaluated the economic impact of social distancing by comparing jobs that can be performed remotely to those that can only be in-person, where the job type classification is made using survey data from O\*NET. They found the former tends to pay higher than the latter. Both studies suggest the pandemic had an impact on groups of all income levels. It is reasonable to conjecture that there is a corresponding alteration of cities’ night light luminosity resulting from the halt in economic performance.

The main hypothesis of this study is that government-enforced lockdown measures impede consumption and investment activities and slow economic growth, which result in the dimming of lights. I aim to investigate whether this change is present in Milan, Italy in 2020. Milan is chosen as the treatment unit because it was the first major city that implemented strict lockdown measures outside of mainland China. To draw a conclusion that the difference between the treated and counterfactual Milan is due to the lockdown policy, there must be a distinguishable gap between the two, and this gap should be the most significant among all the control units. If a change in night light luminosity exists as a result of the policy intervention and aligns with the GDP outcome, I conclude that the government issued lockdown measures had a discernible impact on the region’s economic performance, and nighttime lights serve as a reliable indicator for conducting such analysis.

Synthetic controls method is used to construct the counterfactual night light image of Milan and the counterfactual quarterly GDP data for Italy. First, I apply an extension of classical synthetic control on the distribution of night lights for Milan in each month, and construct the counterfactual image using the nine control units. Second, I apply the classical synthetic control on quarterly GDP per capita to obtain the counterfactual data for Italy had it not gone through any lockdown measure. The treatment group is then compared to the counterfactuals, and their differences are recorded. To arrive to a causal conclusion, I perform permutation tests for both procedures. Should the gap be significant, that is, be a result of the policy intervention, the recorded difference would be the most extreme among all control units when the controls are treated like the treatment group.

Finally, the control units used to construct counterfactual Milan include nine cities: Ankara and Istanbul (Turkey), Boa Vista (Brazil), Dodoma (Tanzania), Lilongwe (Malawi), Minsk (Belarus), Osaka (Japan), Seoul (South Korea), and Taipei (Taiwan, China). All of them did not have any government-issued lockdown measures implemented during 2020.<sup>1</sup> Other criterion for the selection of control units include satellite image availability, policy consistency within the country, et cetera. The details for the selection process of controls are listed in Appendix [A.1](#).

---

<sup>1</sup>Japan issued a “state of emergency” that spread to the whole country on April 16th, 2020. Since it was not enforced by the government, Osaka is not considered having a lockdown in this study.

## 1.1 Background on Italy’s Lockdown

On February 21st, 2020, Lombardy, the region in which Milan is the capital of, published an ordinance that suspended all public events, commercial activities not of public utility, work, play, and sporting activities, and ordered the closure of schools in ten municipalities<sup>2</sup>. On February 23rd, a new decree-law was implemented that furthered the closure of schools of all levels and institutes, and all activities commercial. It also suspended regional railway services with the suppression of stops at some stations. The government declared the deployment of armed forces to enforce the quarantine of specific municipalities. Individuals who violate the blockage were subject to penalties ranging from a fine of 206 euros to a maximum imprisonment of 3 months. The government then announced on March 4th that the measures are valid throughout the national territory.

A new decree was issued by the Prime Minister on the night of March 7-8th. The decree imposed more stringent measures in Lombardy and 14 provinces in the Centre-North, affecting a total of 16 million people. The decree also included measures that applied to the entire country. The new decree prohibited movement to and from the restricted territories, as well as movement within those territories. Milan, along with 25 other provinces in five regions<sup>3</sup> went into phase 1 lockdown in March 9th that lasted until May 3rd. More stringent measures were implemented during this period.

Italy went into a gradual easing of the previous containment measures (“phase 2”) as new cases start to descent in May. This included some partial reopening of public services. Museums and retail services, as well as bars and restaurants resumed throughout Italy on May 18th. Schools remained in remote teaching until the next school year. More easing of measures started on June 11th that allowed access to indoor recreational activities. However, towards the end of 2020 cases started to increase, and previous containment measures resumed on October 8th with a state of emergency extended until January of 2021.

Based on the aforementioned timeline, I consider March 8th the beginning of the policy intervention, and February the last month in the pre-treatment period.

## 1.2 Literature review

In their study, [Henderson et al. \(2012\)](#) provide reasons for why satellite-captured images of nighttime lights can serve as a useful proxy for GDP when measuring economic growth. First, night light images captured by satellites reflect both outdoor and some indoor lighting. Second, real GDP is usually badly measured in developing countries for the lack of consistent domestic price indices. Third, cross-country comparisons are additionally challenging without reliable purchasing power parity (PPP) exchange rates. Moreover, GDP is typically unavailable at the sub-national level or in a timely fashion. Other proxies such as electronic bills, as used by the IMF and the Federal

---

<sup>2</sup>These municipalities are: Codogno, Castiglione d’Adda, Casalpuusterlengo, Fombio, Maleo, Somaglia, Bertonico, Terranova dei Passerini, Castelgerundo and San Fiorano

<sup>3</sup>These regions are: Piedmont, Lombardy, Emilia Romagna, Veneto, Brands

Reserve, only cover limited areas of the world and are either not readily accessible for low-income countries, or not available in a timely manner. The authors demonstrate that nighttime lights overcome all those obstacles in that it is consistently measured and usually available on a monthly basis. Importantly, they show that rising income levels correspond to an increase in light usage per capita, which lead to brightening of night lights.

Despite the various advantages of night lights over GDP, [Henderson et al. \(2012\)](#) notes the limitations to their use. A particular inadequacy relevant to this study is that night lights tend to underestimate economic downturns as they dim less during such periods than they brighten during times of growth. As a result, we may expect lights in Milan to respond less intensively during 2020 as compared to the actual economic effect of the lockdown policy. Additionally, the response of night lights to short-term economic shocks can be sluggish, and [Henderson et al. \(2012\)](#) only considered long-term impacts for this reason.<sup>4</sup> This paper distinguishes from [Henderson et al. \(2012\)](#) in that it focuses on evaluating the changes in night light resulting from a short-term policy intervention, rather than long-term changes in economic growth.

[Beyer et al. \(2023\)](#) used a difference-in-differences approach to study the impact of varying containment measures on night light intensity in districts of India. Combined with other sources, such as Facebook mobility data and surveys, and compared to districts with the least restrictions, they found that the night light intensity for districts with strictest restrictions is 12.4% lower, and that for intermediate restrictions is 1.7% lower. Their findings further confirmed the correlation between change in nighttime light luminosity and decrease in business activities as a result of lockdown measures.

[Stathakis et al. \(2021\)](#) examine the change in light emissions in municipalities in Greece before and after the pandemic. They find that the degree of dimming in nighttime lights is not proportional to the severity of the pandemic’s impact. Specifically, they discover that night lights in densely urbanized areas fluctuate less than those in sparsely urbanized areas due to less permanent population. As Milan is a dense metropolitan area with stable resident population and large buildings, their results suggest that a divergence in lights in Milan may not be apparent.

In addition to the impact of government lockdown policies, the pandemic associated voluntary social distancing may also have contributed to economic declines, as noted by [Caselli et al. \(2020\)](#). Looking across 52 countries, they computed the correlation between lockdown severity and GDP forecast errors. The authors suggest that economic activities might not recover until health risks are minimized. Notably, they highlight the potential positive impact of implementing early-stage lockdown measures that effectively curtailed COVID-19 infections, which minimizes the need for voluntary social distancing. This offers an alternative viewpoint for analyzing the correlation between economic performance and lockdown measures. Specifically, by implementing lockdown policy early in time, Milan might benefit from faster economic recovery later in 2020. Japan,

---

<sup>4</sup>Development of the Korean peninsula (1992 - 2008), the Asian financial crisis in Indonesia (1997 - 1998), Rwanda genocide (1993 - 1996), and Madagascar gemstone (1998 - 2003).

South Korea, and Taiwan also implemented monitoring measures that are considered effective in restraining the spread of COVID-19 cases.

While previous research, including [Henderson et al. \(2012\)](#), has used night lights as a predictor for income levels, I study night lights as a response variable to the policy intervention. The duration of the lockdown policy investigated in this paper is much shorter than the interventions examined by [Henderson et al. \(2012\)](#), and there is limited research on how night lights respond to short-term shocks. Furthermore, I employ a methodology, namely synthetic control, that makes it possible to compare the treated unit with its counterfactual at the same time period, and accounts for unobserved trends in night lights over time that are unrelated to the effect of the lockdown measures. This differs from other studies that analyze night lights during the pandemic, such as [Stathakis et al. \(2021\)](#), who compare night lights of Greece over a span of four years from 2017 and 2020. Synthetic controls method also does not require the parallel trend assumption needed in the difference-in-differences framework used by [Beyer et al. \(2023\)](#).

## 2 Data

The satellite images of nighttime light used in this study were obtained from Google Earth Engine, which is provided by the Earth Observation Group at the Payne Institute for Public Policy at the Colorado School of Mines. These images have a resolution of 463.83 meters and are compiled on a monthly basis, making city-month the unit of observation. The period of observation spans 24 months from January 2019 to December 2020. Each pixel in the images has a numeric value representing the monthly average radiance in the `avg_rad` band, composed from the Visible Infrared Imaging Radiometer Suite (VIIRS) Day/Night Band (DNB). The higher the value, the more luminous the pixel. The variable of interest in this study is thus the distribution of those values, named as `avg_rad`, in each picture. The majority of values fall within the range of  $[0, 200]$  during the observation period, as demonstrated in [Table 1](#).

An alternative band called `cf_cvg` (“cloud-free coverage”) in the dataset adjusts for factors that may result in poor image quality, such as natural geography and climate fluctuations. However, due to its narrower range of values ( $[0, 84]$ ) in comparison to `avg_rad`, the changes in light captured by `cf_cvg` are more subtle. Therefore, I choose to use `avg_rad` as the metric for nighttime light luminosity in this study.

Night light image of 10 cities are obtained for Milan, Ankara, Istanbul, Boa Vista, Dodoma, Lilongwe, Minsk, Osaka, Seoul, and Taipei. Each unit of observation is a monthly composite image of a city’s nighttime lights. The observation period spans from January 2019 to December 2020, totaling 24 months. The pre-treatment period starts from January 2019 to February 2020 as Milan’s official lockdown started in early March. The post-treatment period covers the remaining 10 months from March to December 2020.

[Table 1](#) presents the distribution of `avg_rad` in December 2019 for Milan and three selected

Table 1: Distribution of Night Light Luminosity for Selected Cities, December 2019

	range	Dodoma	Istanbul	Milan	Seoul
	(-1,19]	100%	24.2%	51.2%	13%
	(19,39]	0%	18.3%	29.2%	18.7%
	(39,59]	0%	19.9%	15%	25.4%
	(59,79]	0%	20.1%	3.7%	29.6%
	(79,99]	0%	11.9%	0.5%	9.4%
	(99,119]	0%	3.2%	0.2%	2.6%
	(119,139]	0%	1.2%	0.1%	0.5%
	(139,159]	0%	0.6%	0.1%	0.2%
	(159,179]	0%	0.3%	0%	0%
	(179,199]	0%	0.2%	0%	0.3%
Pop. density (per sq. km)		184	9910	2045	15138
GDP per capita (2019 \$)		1052	9103	33673	31902

control cities that represent different level of night light luminosity, which are Dodoma, Istanbul, and Seoul. Population density<sup>5</sup> as well as GDP per capita gathered from the World Bank database are provided as reference. We can inferred from its night light luminosity distribution that Dodoma has lower level of development compared to the other three cities. This inference is consistent with the fact that Dodoma has lower GDP per capita among the four cities. Figure 1 is a visual representation of Table 1, showing the cumulative distribution of night light luminosity for the four cities. The luminance value `avg_rad`, ranging from 0 to 200, is scaled between 0 and 1 on the x-axis. The figure indicates that Istanbul and Seoul have relatively similar distributions of luminosity, possibly because of their comparable population densities. Meanwhile, Dodoma has the lowest luminance, which aligns with that presented in Table 1. The quantile functions, the inverse of the cumulative distribution function in Figure 1, are used as the probabilistic measure to perform synthetic control.

In addition to night light luminosity, this study also employs classical synthetic control on three common economic indicators as measures of economic performance: quarterly GDP per capita<sup>6</sup>, quarterly employment rate<sup>7</sup>, and quarterly unemployment rate<sup>8</sup>. The quarterly GDP per capita, in current US dollars, is estimated by adjusting nominal GDP using purchasing power parity (PPP), and dividing the result by the current population. Due to less frequent data availability, quarterly data is chosen instead of yearly to obtain more observations within a relatively short period of time.

<sup>5</sup>Data obtained from [Center For International Earth Science Information Network-CIESIN-Columbia University \(2017\)](#)

<sup>6</sup>Data obtained from [U.S. Bureau of Economic Analysis \(2023\)](#)

<sup>7</sup>Data obtained from [OECD \(2023a\)](#)

<sup>8</sup>Data obtained from [OECD \(2023b\)](#)

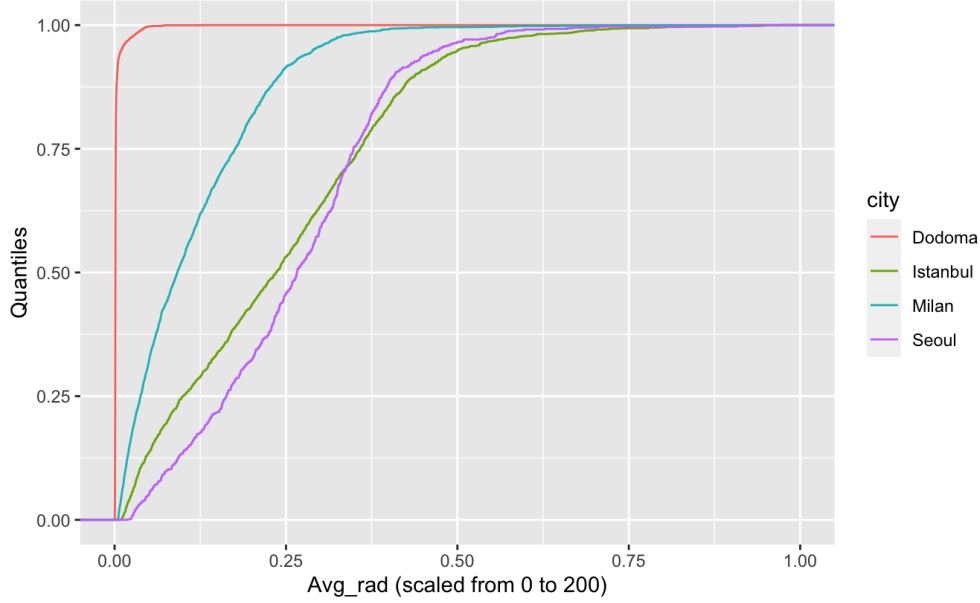


Figure 1: Cumulative Distribution of Night Light Luminosity for Selected Cities, December 2019

Each quarter contains three months, with the first quarter being January, February, and March. Given the policy took place in March, the pre-treatment period spans 13 quarters from 2017 Q1 to 2020 Q1, and the post-treatment period consists of three quarters from 2020 Q2 to 2020 Q4. Moreover, out of the ten countries involved in the study, only Italy, Japan, Korea, and Turkey have data available for quarterly employment and quarterly unemployment rates. As a result, the analysis encompasses a total of 64 observations, covering a 16-quarter observation period across four countries. Figure 2 illustrates the quarterly trend of GDP per capita during the observation period for the countries of interest. It is noticeable that all four countries experienced a drop (perhaps less significant for Korea) from 2020 Q1 to Q2, which was when the COVID-19 pandemic hit the world.

### 3 Method

When studying causal impacts of a policy intervention, we are interested in estimating the effect of the intervention on the outcome of interest for the treated unit in post-treatment period. Randomized control trials allow us to conduct such analysis with experiments. With observational data, one widely used technique is difference-in-differences, which calculates the difference in the variable of interest between a treatment group and a control group. Control group is selected satisfying the parallel trend assumption, that the difference between the treatment and control group in the pre-treatment period is constant over time. Diff-in-diff eliminates biases caused by inherent differences between the treatment and control groups, as well as external factors influencing the outcome of interest. However, the parallel trend assumption is hard to fulfill in non-randomized settings.



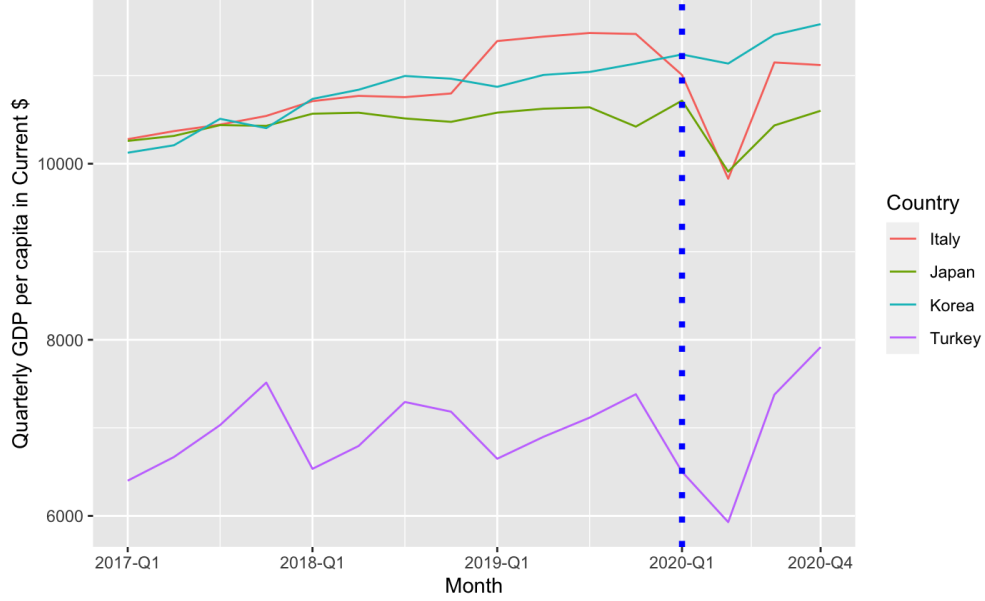
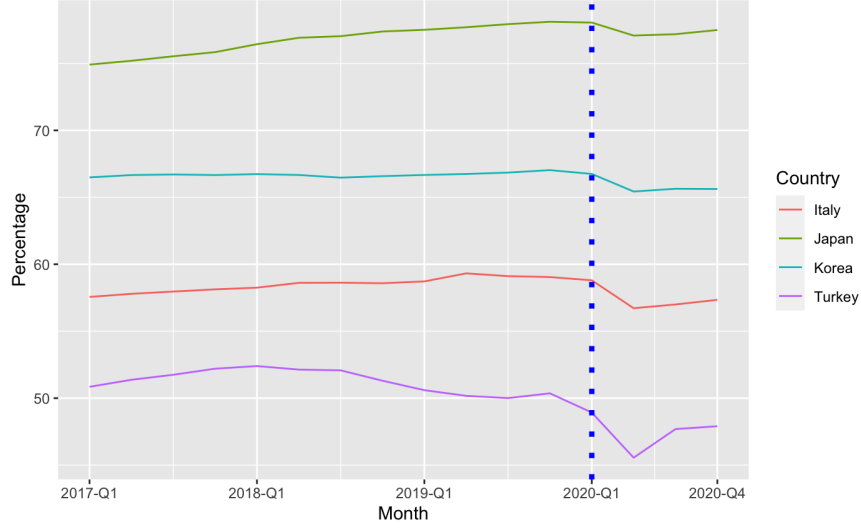


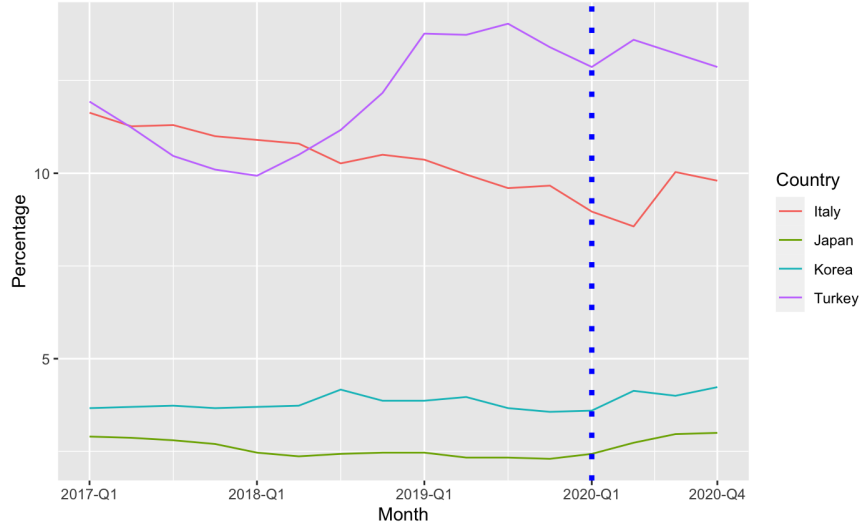
Figure 2: Nominal GDP per capita trend for Italy and Four Control Countries (2017 Q1 - 2020 Q4)

Synthetic control method addresses this limitation by constructing a synthetic control group that mimics the unobserved potential outcome, i.e. the outcome had the unit not gone through the treatment. The synthetic control group is a convex combination of multiple control units, with the weights chosen to minimize the difference between the control group and the treated unit with respect to the outcome of interest in the pre-treatment period. The resulting optimal weights are then used to construct the counterfactual unit of interest, when it is in the absence of the policy intervention. The outcome of interest, GDP for instance, is the desired characteristic of the treated unit that we are interested in, and multiple predictors can be used in calculating the optimal weights. SCM has been widely used in studying the impact of treatment policies, and is particularly useful when the policy takes place at an aggregate level that affect a small number of units (Abadie et al., 2010).

This paper employs the distributional synthetic control (DSC) method recently introduced by Gunsilius (ming), which is an extension of the classical synthetic control method that constructs the counterfactual distribution of the variable of interest when data is available at fine granularity. Specifically, the outcome of interest in this study is the distribution of monthly composite night light luminosity (represented by the distribution of `avg_rad`) in Milan. In addition, classical synthetic controls is performed on quarterly GDP per capita, along with employment rate and unemployment rate as predictors, to estimate the impact of the lockdown policy on GDP in Milan.



(a) Employment Rate



(b) Unemployment Rate

Figure 3: Trend in Employment Rate and Unemployment Rate for Italy and Four Control Countries (2017 Q1 - 2020 Q4)

### 3.1 Distributional Synthetic Control

Distributional synthetic control considers the distribution of the outcome variable in the pre-treatment period, and constructs a counterfactual distribution that matches the distribution of the treatment unit as closely as possible. The objective is to replicate the quantile function associated with the treated unit by a weighted average of quantile functions of the control units. This is done using a weighted combination of the outcomes of the control units, where the weights are chosen to minimize the distance between the distribution of the control units and the distribution of the treatment unit across the pre-treatment period.

Quantile functions are used to represent the distribution so that comparison of distributions with different supports is possible. In particular, a single weight is computed for the entire quantile function, allowing the optimal weight to be independent of the choice of the point within the distribution (Gunsilius, ming). For unit  $j$  in period  $t$ , each observation is assigned a weight  $\lambda_{j,t}^*$  that best approximates the target (treatment) unit. The optimal weights  $\lambda_t^* = [\lambda_{1,t}^* \dots \lambda_{j,t}^* \dots]^T$  are obtained by minimizing the difference between quantile functions of the treated unit and the weighted average of control units, for each  $t \leq T_0$ .

The difference, or distance, between two distributions that we aim to minimize is represented by the squared Wasserstein distance,  $W_2$ , which simplifies the optimization problem to a regression problem (Gunsilius, ming). For two probability measures  $P_1$  and  $P_2$  with their respective quantile functions  $F_1^{-1}$  and  $F_2^{-1}(q)$ ,  $W_2$  is defined as

$$W_2(P_1, P_2) = \left( \int_0^1 |F_1^{-1}(q) - F_2^{-1}(q)|^2 dq \right)^{1/2}. \quad (1)$$

Let  $F_1^{-1}(q) = F_{M,t}^{-1}(q)$  be the distribution for target, and  $F_2^{-1}(q)$  be that for the weighted average of the control units. Then the weights for control units at each time period  $t$  are obtained through solving Equation 2:

$$\lambda_t^* = \arg \min_{\lambda \in \Delta^J} \int_0^1 \left| F_{M,t}^{-1}(q) - \sum_{j \in J} \lambda_{j,t} F_{j,t}^{-1}(q) \right|^2 dq, \quad (2)$$

subject to  $\lambda_{j,t}^* \geq 0$ , and  $\sum_{j \in J} \lambda_{j,t}^* = 1$ ,  $\forall j, t$ .

### 3.2 Applying DSC to Night Light Images

The outcome of interest is the distribution of night light luminosity, formed by numbered pixels in the satellite image. Each image represents a city in a month. And each pixel has a number attached that represents the luminance (`avg_rad`) of the area covered over the month, standardized to 463.83 meters. The pixels also include longitudinal and latitudinal data. When stacking the pixels into a distribution, the exact location of each pixel in the image is ignored. In other words, having a bright spot on the upper right corner of the image is the same as having that spot on the lower left corner, as long as the distribution formed from the two images remain the same. Since the focus is on the total change in brightness of the city, shifts of brightness<sup>9</sup> is of no influence to the conclusion made. To recover the image for later presentation, I use geographic coordinates attached to the pixels. Naturally, differences in natural geography and size of metropolitan area result in difference in the lengths of the vectors of `avg_rad`, which is not a concern as we are comparing the quantile function, not the cumulative distribution, of the variable.

---

<sup>9</sup>One could interpret it as shift of city center.

Let  $x$  represent the quantile of the `avg_rad`. Let  $F$  be the cumulative distribution function for `avg_rad`, and  $F^{-1}$  the quantile function. Let  $F_{M,t}^{-1}$  be the quantile function for Milan in month  $t$ , and  $F_{j,t}^{-1}$  be that for the  $j$ th control unit in month  $t$ , for all  $j \in J$  and  $t \in T$ , with  $J = \{1, \dots, 9\}$  be all control units and  $T = \{1, \dots, 24\}$  be all periods covered by the data. Lastly, let  $\tilde{F}_{M,t}^{-1}$  be the quantile function for counterfactual Milan in month  $t$ , and let  $T_0 = 14$  be the last period before the start of the policy intervention.

For  $t > T_0$ , the counterfactual distribution of Milan in quantile function at a given month  $t$  is acquired as

$$\tilde{F}_{M,t}^{-1}(x) = \sum_{j \in J} \lambda_j^* F_{j,t}^{-1}(x), \quad (3)$$

with each control unit getting one optimal weight,  $\lambda_j^* = \frac{1}{14} \sum_{t \leq T_0} \lambda_{j,t}^*$ , which is the simple average of the optimal weights obtained in each of the 14 months in the pre-treatment period, and  $\lambda_{j,t}^* \in \lambda_t^*$ .

Finally, the  $W_2$  distance between two quantile functions of night light luminosity for counterfactual Milan and treated Milan at a given month  $t$  is calculated using Equation 1.

### 3.3 Permutation Test

To see if the difference observed between counterfactual and treated units has a causal relationship with the treatment policy, a placebo permutation test is performed by applying the above procedure on each of the nine controls, pretending each control unit is the treatment group, and use all other units as controls. If an actual treatment effect was present, the estimated effect measured in  $W_2$  distance is expected to be the most extreme for the actual treated unit, Milan.

Let  $\lambda_k^*$  be the set of optimal weights assigned to the new control group when the  $k$ th unit is treated as the treatment unit. Algorithm 1, one that described in [Gunsilius \(ming\)](#), outlines the steps taken in the placebo permutation test.

---

#### Algorithm 1 Placebo Permutation Test

---

```

1: for each unit  $k \in \text{control cities}$  do
2:   for each month  $t \leq T_0$  do
3:     obtain and record optimal weights,  $\lambda_{k,t}^*$ , using Equation 2
4:   end for
5:   compute the overall optimal weights across pre-treatment periods:
6:    $\lambda_k^* = \frac{1}{14} \sum_{t \leq T_0} \lambda_{k,t}^*$  ▷ pre-treatment period contains 14 months.
7:   for each month  $t > T_0$  do
8:     compute  $W_2$  barycenter using the weights  $\lambda_k^*$  and Equation 3 to obtain  $\tilde{F}_{k,t}^{-1}(x)$ 
9:     record  $W_2$  distance  $d_{j,t} := \int_0^1 \left| F_{k,t}^{-1}(q) - \tilde{F}_{k,t}^{-1}(x) \right|^2 dq$ 
10:  end for
11: end for

```

---

### 3.4 Applying Classical Synthetic Control to GDP

GDP is used as a reference outcome in comparison to the changes in night light luminosity. I use the `synth` package in R, developed by [Abadie et al. \(2011\)](#), to perform classical synthetic control.

The procedure is analogous to that of DSC. The set of weights assigned to the control units are  $W = [w_1, \dots, w_J]^T$ , denoted as `w.weights` in Table 2 below. Let  $\mathcal{W}$  be the set of weights satisfying  $w_j \geq 0, \forall j \in J$ , and  $\sum_{j \in J} w_j = 1$ . Then,  $W^*$  is obtained as

$$W^* = \arg \min_{W \in \mathcal{W}} \|X_0 - X_J W\|_V = \arg \min_{W \in \mathcal{W}} \sqrt{(X_0 - X_J W)^T V (X_0 - X_J W)}, \quad (4)$$

where  $X_0$  is a matrix of size  $(k \times 1)$  representing the  $k$  predictors for the treated unit<sup>10</sup>, and  $X_J$  is the matrix of size  $(k \times J)$  representing the  $k$  predictors for the  $J$  control units.<sup>11</sup>  $V$  is some symmetric and positive semi-definite matrix of size  $(k \times k)$  that assign weights to the  $k$  predictors in  $X_0$  and  $X_J$  depending on their predictive power on the outcome<sup>12</sup>, and is denoted as `v.weights` in Table 3 below. Let  $Z_0$  be the vector of outcome variable for the treated unit over pre-treatment period, and  $Z_J$  be the analogous matrix for the control units. Let  $\mathcal{V}$  be the set of all symmetric and positive semi-definite matrices. The optimal weights of predictors,  $V^*$ , are those that minimizes the mean squared prediction error of the outcome variable over the pre-treatment periods ([Abadie et al., 2011](#)):

$$V^* = \arg \min_{V \in \mathcal{V}} (Z_0 - Z_J W^*(V))^T (Z_0 - Z_J W^*(V)), \quad (5)$$

where  $W^*(V)$  is given by Equation 4. The `synth()` function solves for this nested optimization problem of Equation 5.

## 4 Result

### 4.1 Empirical DSC Result of Milan

Figure 4 displays the preliminary outcome of applying distributional synthetic control to the night light images of Milan in December 2019 (before treatment) and December 2020 (after treatment). The two months are selected because they are exactly a year apart, ruling out any potential seasonal influence on the images captured; and December 2019 is the latest month before the treatment policy takes place that allows for a year of comparison. Figure 4b and 4d are generated using a weighted average of the nine control units at December 2019 and December 2020, respectively. The same set of optimal weights is used for the two images, which is obtained from minimizing the difference in distributions between the target and the controls in December 2019. As shown in the figures, there is a high degree of similarity between 4a and 4b, indicating a well-approximated luminosity distribution. Figure 4d is then generated using the same set of weights used to construct Figure

<sup>10</sup>In this case, it is Italy.

<sup>11</sup>Here,  $J = 3$ : Turkey, Japan, and Korea.

<sup>12</sup>In this case, it is quarterly GDP per capita.

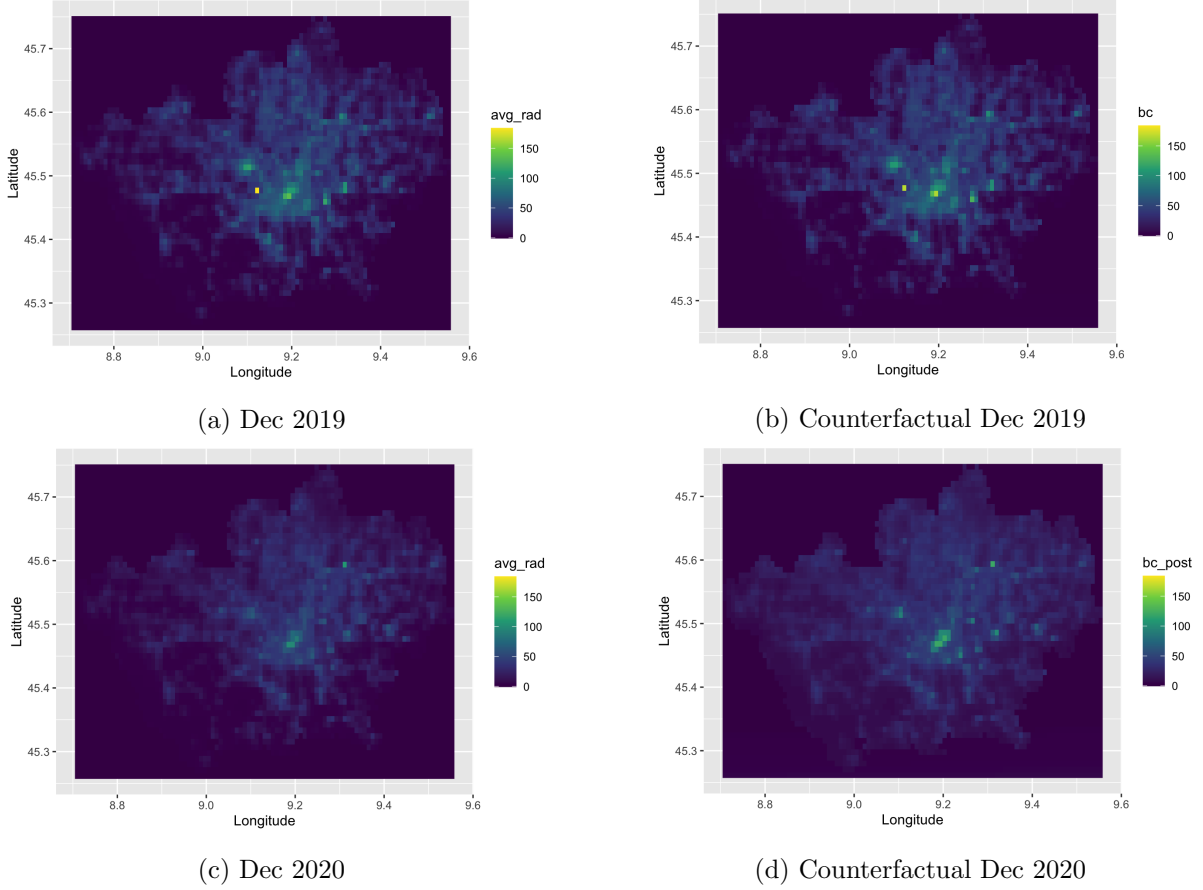


Figure 4: Night Lights of Milan in December 2019 and December 2020 with their respective counterfactual comparisons

4b. While it still closely resembles Figure 4c, there is small deviation that may be attributed to the effect of the treatment policy.

To study the treatment effect of lockdown policy across the entire post-treatment period, that is March to December of 2020, I use  $W_2$  distance between the distributions of `avg_rad` for treated and counterfactual Milan in each of the 24 periods to represent the discrepancy. The result is given in Figure 5.  $T_0$  is at the February 2020, the last month in the pre-treatment period, and is marked as the dotted blue line. We see that the  $W_2$  distance remains small and stable throughout the pre-treatment months with the exception of one month (February 2019)<sup>13</sup>. This provides evidence that the control group and the set of optimal weights chosen approximates Milan’s night light luminosity well. In the post-treatment period to the right of the dotted line, the  $W_2$  distances become larger and irregular, indicating discrepancies between the distributions of `avg_rad` for treated and counterfactual Milan. The post-treatment period suggests that there is likely a change in Milan’s night lights luminosity after implementing the lockdown.

<sup>13</sup>As the special case does not repeat itself, I opt not to dedicate my efforts towards its explanation.

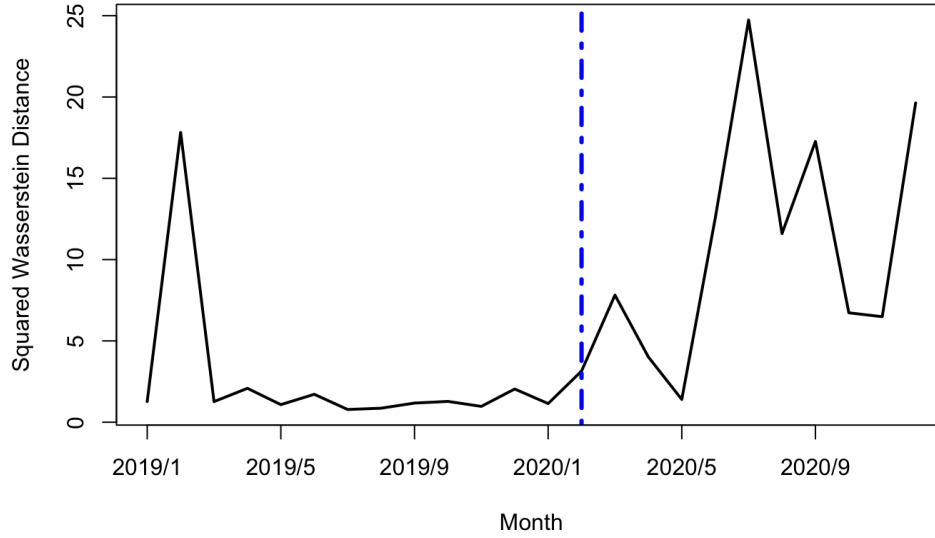


Figure 5: Squared Wasserstein Distance between Counterfactual Milan and Actual Milan from January 2019 to December 2020

## 4.2 Permutation Test

Should the discrepancy observed in Figure 5 be a result of the lockdown measure, we would expect the  $W_2$  distance for Milan to be the most extreme among the control units post-treatment. However, as Figure 6 shows, the fluctuation in  $W_2$  between actual and counterfactual for Milan is almost negligible in comparison to the grey lines, which represent the control units when performed with the same procedure. This fails to support the existence of a treatment effect on the city’s night lights resulting from the implementation of the lockdown policy. To examine whether the absence of a significant difference is due to a lack of change in economic activity or the inadequacy of night lights as an indicator, I perform classical synthetic control on Italy’s GDP measure in the next section.

## 4.3 Classical Synthetic Control

The classical synthetic control method is employed on three widely used economic indicators: quarterly GDP per capita, quarterly employment rate, and quarterly unemployment rate. The variable of interest is GDP per capita, and I use quarterly employment rate and quarterly unemployment rate as additional predictors. The unit of observation becomes country-quarter. The treated unit is Italy and the controls are Japan, Korea, and Turkey<sup>14</sup>.

Similarly, to provide evidence of a substantial treatment effect of the lockdown policy on quarterly GDP per capita, it is needed to observe high similarity between actual and synthetic GDP

<sup>14</sup>Other control units from previous section are dropped due to data availability on quarterly GDP.

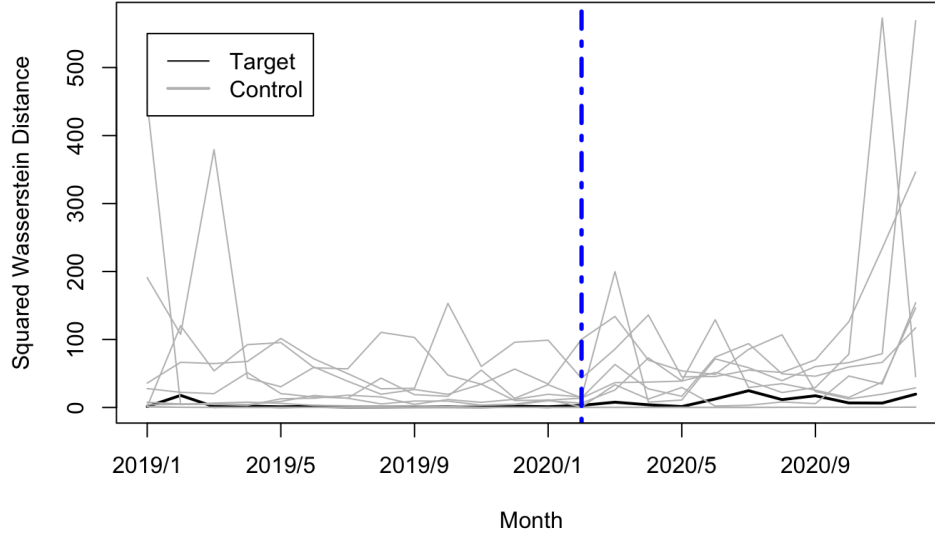


Figure 6: DSC Placebo Permutation Test: Difference in Night Light Luminosity Distribution for Milan and Nine Control Cities

prior to the intervention, followed by a significant divergence between the two trajectories after the intervention. The resulting weights of potential controls ( $W^*$ ) are given in Table 2. We see that Korea contributes roughly 96%, making it the major donor for constructing synthetic Italy. Similarly, the optimal weights of predictors ( $V^*$ ), as shown in column 1 of Table 3, shows that only quarterly GDP pc is used, and this sacrifices the prediction accuracy for employment and unemployment rates as presented in columns 2 and 3 of Table 3. Figure 7 shows the trend and gap in GDP per capita for Italy and synthetic Italy. The x-axis represents observation periods (in quarters) in simplified notation: 0 represents the onset of the treatment in 2020 Q1, and  $-12$  represents start of the treatment period in 2017 Q1. We notice that the synthetic GDP does not approximate the actual trend well prior to the intervention, especially from 2019 Q1 ( $-4$  on the axis) to 2019 Q4 ( $-1$  on the axis). This misalignment is more prominent in 7b which shows the gap between treated and synthetic Italy over time (actual - synthetic). Nonetheless, a decrease in GDP is observed in the first quarter post-treatment compared to the synthetic GDP of Italy.

Correspondingly, a placebo permutation test is performed on quarterly GDP per capita for all three control units. The result in difference between actual and synthetic GDP is shown in Figure 8.<sup>15</sup> We see that the drop in GDP in 2020 Q2 is not the most extreme for Italy, suggesting no significant treatment effect of lockdown policy on GDP is present.

<sup>15</sup>The grey curve that is markedly below the three other curves is the result when Turkey is treated as the treatment unit. Due to the small number of control units, the procedure failed to construct a synthetic Turkey that is close to the actual data, and it assigned weight = 1 to Korea. As a result, this grey curve is effectively the difference in GDP per capita between Turkey and Korea.



Table 2: Weights for Control Units

	w.weights
JPN	0.029
KOR	0.962
TUR	0.010

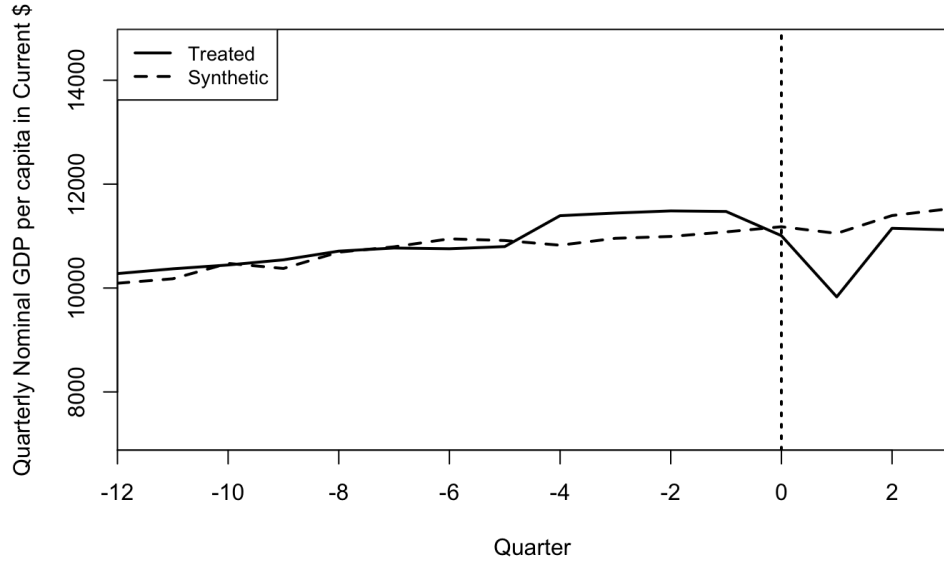
Table 3: Weights for Predictors and Synthetic Output

	v.weights	Treated	Synthetic	Sample Mean
Employment Rate	0	58.223	66.622	64.569
Unemployment Rate	0	10.29	3.875	6.205
Quarterly GDP pc	1	10848.303	10841.887	9436.909

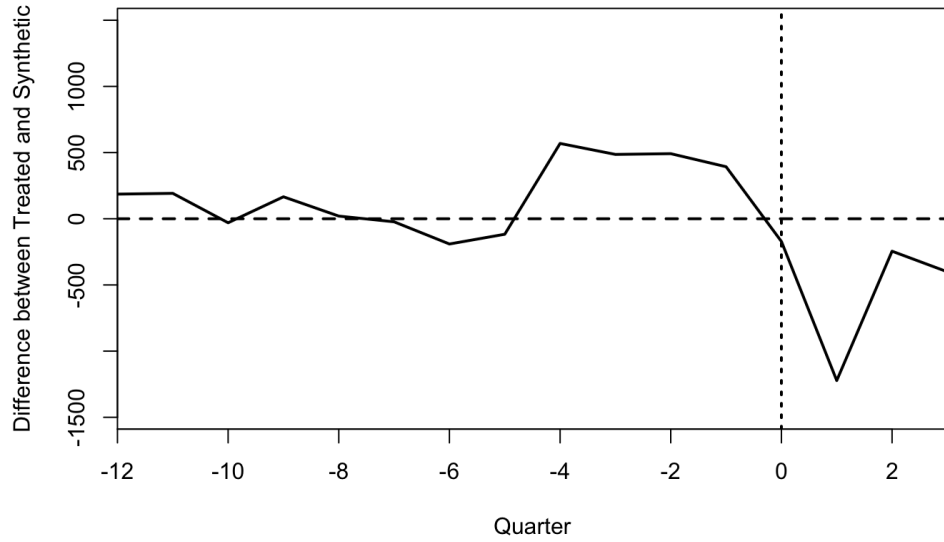
## 5 Discussion

Satellite images of cities provide a distinctive perspective on human settlements, enabling the opportunity to study economic activities without political boundaries worldwide. This paper investigates the impact of the COVID-19 lockdown policy implemented in Milan on the luminosity of night lights. It uses distributional synthetic control on satellite images to evaluate the treatment effect on night lights associated with the policy intervention. In addition, classical synthetic control is performed on quarterly GDP per capita. The results reveal no significant differences in both night light luminosity and GDP in the post-treatment period, indicating that the lockdown measures did not have a significant economic impact in Milan.

Multiple explanations are possible for the findings of this paper. First, as noted by [Stathakis et al. \(2021\)](#), densely populated urban regions tend to have a more consistent brightness at night compared to sparsely populated areas. Milan, as an agglomeration of high-rise with developed infrastructure, is likely to have more stable luminosity at night over short periods of time. Besides, given the results of night light luminosity is consistent with that of GDP, the lockdown measures may not have had a significant negative impact on the economy. Other factors unrelated to government protocols, such as public perceptions of health risks, might also be at play. As highlighted by [Caselli et al. \(2020\)](#), voluntary social distancing without government mandates can have a negative impact on the local economy. Therefore, it is conceivable that the prompt enforcement of strict lockdown measures in early 2020 reduced residents’ health-related concerns in Milan as compared to areas without government policies, thereby expediting the recovery of business activities.



(a) Trends



(b) Gap

Figure 7: Quarterly GDP per capita between Actual and Synthetic Italy (2017 Q1 - 2020 Q4)

Finally, the method used in this paper could also benefit from improvements. For instance, the distributional synthetic control method can be expanded to a multivariate version, which would allow for more variables to be included in the calculation of optimal weights ([Gunsilius et al., 2022](#)). In the context of this study, it would be beneficial to include population density and elevation, in addition to average radiance, to better control for the factors that influence night lights. Moreover, the selection of control regions could be bettered by choosing areas that are more economically

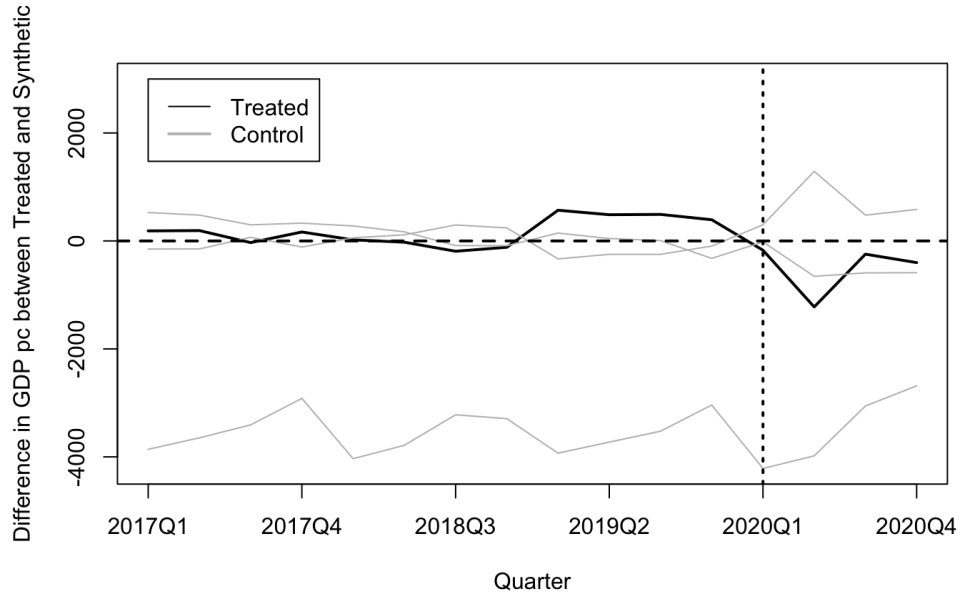


Figure 8: Classical SCM Placebo Permutation Test: Gap between Actual and Synthetic Quarterly GDP per capita for Italy and Three Control Countries

and politically similar to Milan, as a developed region may not be adequately approximated by less developed ones. It is worth noting that the unique circumstances of the global pandemic made the selection of control regions particularly challenging, as only a few areas did not implement any government policies in response. Another potential approach to compensate for the limitations of the control regions is to incorporate more pre-treatment periods to improve the calculation of optimal weights. These improvements could enhance the accuracy and reliability of the results obtained from the method.

## 6 Acknowledgement

I would like to express my heartfelt gratitude to everyone who has helped me during the completion of this thesis. I'm especially indebted to Professor Florian Gunsilius, my advisor, who inspired the topic of this thesis and provided unwavering support in coding, countless discussions, and invaluable encouragement that deepened my interest in the field of economics.

I am also grateful to Rex Hsieh for his extensive assistance through discussions and insightful comments.

I would like to acknowledge the assistance of Linsong Liu, who helped with the collection of satellite images.

I would also like to thank Pietro Tommaso Bragante, for his valuable observations on the pandemic lockdown in Italy, and Jojo Lee, for the many helpful discussions.

Lastly, I would like to extend my gratitude to my parents, whose love are with me in whatever I pursue.

## A Appendix

### A.1 Choice of Controls

The regions with no lockdown policy in 2020<sup>16</sup> are:

- Belarus;
- Brazil (Roraima, Rondônia);
- Burundi;
- *Cambodia*;
- *East Timor*;
- Iceland;
- Japan;
- *Malawi*;
- Nicaragua;
- South Korea;
- Sweden;
- Taiwan;
- Tanzania;
- *Turkey*;
- United States (Arkansas, Iowa, Nebraska, North Dakota, South Dakota, Wyoming);
- Uruguay.

Among them, Cambodia, East Timor, Malawi, and Turkey, did not impose lockdown measures until early 2021, which is outside of the period of study in this paper. Meanwhile, Japan, South Korea, and Taiwan rapidly and consistently implemented highly organized mass testing, contact tracing, public messaging, and selective quarantining. Sweden is the only country in the European Union that did not implement lockdown measures; however, it is dropped from the control list due to missing satellite image in the observation period. Cambodia and Iceland are also not included in the control list for a similar reason.

---

<sup>16</sup>The following information is referencing [Wikipedia contributors \(2023\)](#).

Another concern for the selection of controls is the comparability of economic factors. For this reason, Burundi, East Timor, Nicaragua, and Uruguay are not included as control units. The United States present a unique challenge due to the diversity in policies across different regions. While some regions had strict lockdown measures, others had none at all. Since GDP is measured nationally, it is difficult to capture the effects at a local level. Therefore, U.S. states were not included as control units in this study.

## References

- Abadie, A., A. Diamond, and J. Hainmueller (2010). Synthetic control methods for comparative case studies: Estimating the effect of california’s tobacco control program. *Journal of the American statistical Association* 105(490), 493–505.
- Abadie, A., A. Diamond, and J. Hainmueller (2011). bsynth/b: Anir/ipackage for synthetic control methods in comparative case studies. *Journal of Statistical Software* 42(13).
- Beyer, R. C., T. Jain, and S. Sinha (2023). Lights out? covid-19 containment policies and economic activity. *Journal of Asian Economics*, 101589.
- Caselli, F., F. Grigoli, W. Lian, and D. Sandri (2020). The great lockdown: dissecting the economic effects. *World economic outlook* 65, 84.
- Center For International Earth Science Information Network-CIESIN-Columbia University (2017). Gridded population of the world, version 4 (gpwv4): Population density, revision 11.
- Chetty, R., J. N. Friedman, N. Hendren, M. Stepner, et al. (2020). The economic impacts of covid-19: Evidence from a new public database built using private sector data. Technical report, national Bureau of economic research.
- Dingel, J. I. and B. Neiman (2020). How many jobs can be done at home? *Journal of Public Economics* 189, 104235.
- Gunsilius, F. (Forthcoming). Distributional synthetic controls. *Econometrica*.
- Gunsilius, F., M. H. Hsieh, and M. J. Lee (2022). Tangential wasserstein projections. *arXiv preprint arXiv:2207.14727*.
- Henderson, J. V., A. Storeygard, and D. N. Weil (2012). Measuring economic growth from outer space. *American economic review* 102(2), 994–1028.
- OECD (2023a). Employment rate. accessed on 18 March 2023.
- OECD (2023b). Harmonised unemployment rate (HUR). accessed on 18 March 2023.
- OECD (2023c). Ppps and exchange rates. accessed on 29 March 2023.
- Stathakis, D., L. Liakos, and P. Baltas (2021). Covid-19 pandemic assessment by night-lights. In *2021 IEEE International Geoscience and Remote Sensing Symposium IGARSS*, pp. 6801–6804. IEEE.

U.S. Bureau of Economic Analysis (2023, April). Quarterly gross domestic product [gdp]. accessed on 29 March 2023.

Wikipedia (2023). Gestione della pandemia di COVID-19 in Italia — Wikipedia, the free encyclopedia. <http://it.wikipedia.org/w/index.php?title=Gestione%20della%20pandemia%20di%20COVID-19%20in%20Italia&oldid=132684874>. Online; accessed 31 March 2023.

Wikipedia contributors (2023). Covid-19 lockdowns by country — Wikipedia, the free encyclopedia. [Online; accessed 7-April-2023].